Feasibility of a low-temperature γ-ray laser

S. V. Karyagin

Institute of Chemical Physics, Academy of Sciences of the USSR, Moscow

A γ-ray laser is not feasible, even at an infinite rate of excitation, if realistic pump thresholds are considered and allowance is made for various losses (spontaneous decay, overheating, etc.). However, such *"in situ"* difficulties connected with the processes occurring in the laser itself can be overcome by measures tending to suppress such losses. The measures suggested in the present paper include anomalous dilution of the active nuclei; line narrowing without external action; two-stage pumping with implantation of the excited nuclei in the first target; rf or optical pulse separation of activation, inversion, and lasing processes; fast active and passive resonant switches or systems of these switches in combination with a controlled traveling pump zone; annular amplification schemes. These measures make it possible to avoid the *"in situ"* difficulties, facilitate various types of controlled pumping and stimulted emission of γ rays, and extend the range of isotopes which can be employed as active media in γ-ray lasers. Such measures can be used also (partly) in γ-ray spectroscopy and they can be stimulated at longer (for example, optical) wavelengths. In justifying these measures, expressions are obtained also for the combined threshold conditions allowing for various losses and a two-stage generalized model is proposed to provide a unified approach for comparing various one- and two-stage pumping schemes. Feasibility of emission of γ-ray π pulses is predicted. Comparative numerical estimates of the parameters of the proposed γ-laser schemes are given for six isotopes, which are regarded as examples.

PACS numbers: 42.55.Bi

One of the problems encountered in considering the feasibility of a γ-ray laser[1-11] is that spontaneous decay destroys population inversion before lasing begins,[12-14] and this gives rise to very stringent threshold conditions.[14] Allowance for superradiance[15,16] makes these conditions less stringent. The best threshold conditions are obtained in γ-ray laser schemes proposed below in which the process of pumping is physically separated into activation and inversion stages (zones), and the transition to the lasing zone is abrupt. This separation makes it possible to optimize separately these three stages, because it weakens the linkage between these stages and the main body of γ-ray laser problems. The absence of overheating destroying an active medium is essential for these easier threshold conditions; at the same time it is a consequence of and a significant characteristic of these conditions.

1. STABILITY OF γ-RAY LASING AND OBSTACLES PREVENTING IT

Let us assume that the active medium of a γ-ray laser is elongated into a filament of length L and diameter $d \ll L$. We shall introduce the longitudinal and transverse τ_1 and τ_2 relaxation times of the active transition e-g of a nucleus R between its upper $|e\rangle$ and lower $|g\rangle$ levels whose populations are n_e and n_g and whose degeneracy multiplicities are G_e and G_g; we shall take the population inversion to be $\Delta = n_e - G n_g$, where $G = G_e/G_g$. If R nuclei are impurities present in a concentration $n \gtrsim n_e + n_g$ in a matrix of lighter nuclei R' of concentration $n' \gg n$, the usual threshold rate condition[1-11] has the form $p > 1$, where $p = \mu_0 L_0$ is the gain at $L = L_0$; $\mu_0 = \sigma_0 \Delta$; $L_0 = 1/\Sigma'$ is the length representing nonresonant losses and equal to the reciprocal of the macroscopic cross section of the losses $\Sigma' \approx n\sigma + n'\sigma'$. Here, σ_0 is the cross section for the stimulated transition e-g; σ and σ' are the cross sections of nonresonant

losses for a narrow γ-ray beam interacting with the R and R' atoms.[1)] Spontaneous decay reduces the initial inversion Δ

$$\Delta(t) = (1+wG)n_e(\eta + e^{-t/\tau_1} - 1), \quad \eta = \Delta/[n_e(1+wG)], \tag{1}$$

to zero in a time $t \approx \tau_1 \eta$. Here, $0 \leqslant w \leqslant 1$ is the branching ratio for the decay of the $|e\rangle$ level in the e-g channel.

During a pump pulse $t_p \gtrsim \tau_1$ (see Sec. 3a) we can expect superluminescence accelerating the decay process by a factor of s_0:

$$s_0 \approx 1 + \frac{1}{8} f_\alpha \left(\frac{d}{\xi L_0}\right)^2 \frac{e^{\mu L}}{\mu L}\left(1 + \frac{2}{\mu L}\right), \quad f_\alpha = w \frac{\tau_2}{\tau_1}\frac{f}{1+\alpha}, \tag{2}$$

where $\mu = \mu_0 - \Sigma'$; $\xi = L/L_0$; $\mu L = \xi(p-1) \gg 1$; f is the Mössbauer factor; α is the conversion coefficient. The other quantities are as follows: $(p\xi)_c$ is the minimum gain threshold below which lasing is in principle impossible;[13-16] $p\xi$ is the initial gain; t_0 is the delay; $t_{1/2}$ is the half-width of the output pulse; c' is the velocity of the γ-ray wave in the medium. It follows from Eqs. (1) and (2) that the inversion $\Delta(t)$ does not decrease because of decay by a factor exceeding $(p\xi)_c/p\xi$ in a time $t_0 + t_{1/2}$ provided the initial inversion is

$$\eta \geqslant \eta_c = \left[1 - \exp\left(-\frac{s_0}{\tau_1}(t_0 + t_{1/2})\right)\right]\bigg/\left(1 - \frac{(p\xi)_c}{p\xi}\right). \tag{3}$$

If $L \lesssim L_0 \ll c'\tau_2/p\xi$ and $\tau_2 \approx \tau_1$, it follows from Refs. 15 and 16 that $(p\xi)_c = 2$ and

$$\frac{1}{\tau_1}(t_0 + t_{1/2}) = (4 + (p\xi)^2)^{-1/2}\ln\left[(1 + 2^{1/2})^2 \frac{(4+(p\xi)^2)^{1/2}+p\xi-2}{(4+(p\xi)^2)^{1/2}-p\xi+2}\right]. \tag{4}$$

Substitution of Eqs. (2) and (4) in Eq. (3) gives the threshold condition $\eta \geqslant \eta_c(p, \xi)$ for relative inversion η. The dependence $\eta_c(p)$ (Fig. 1) is due to the fall of $t_0 + t_{1/2}$ before the minimum, whereas beyond the minimum it is due to a steep rise of the superluminescence noise whose influence at the minimum is negligible:
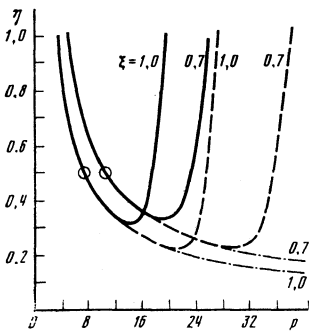
FIG. 1. Thresholds $\eta_c(p,\xi)$ between stable (strong) and unstable (weak) lasing plotted in accordance with Eq. (5). The continuous curves represent normal dilution: $n/n' \approx \sigma'/\sigma$, $L_0 \approx 1$ cm; the dashed curves represent anomalous dilution (Sec. 2), $L_{0b} \approx 10^2$ cm, $B \approx 10^{-3}$; the chain curves are plotted ignoring the superluminescence noise: $d \approx 10^{-2}$ cm, $f_\alpha \approx 0.1$. At the minima, $s_0 \approx s_{AD} \approx 1 + 0.05$. The circles denote the conditions (38) and (43).
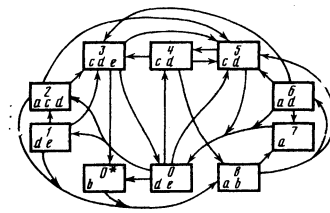

FIG. 2. Mutual enhancement (arrows) in combinations of losses (numbers) suppressing lasing: 1) spontaneous decay; 2) enhancement of spontaneous decay (super-luminescence noise); 3) depletion of population inversion Δ; 4) prethreshold weak (unstable) lasing; 5) deviation from spatial and temporal homogeneity of initial lasing conditions; 6) multimode lasing; 7) fall in accordance with $\sigma_0 \propto f/\Gamma\tau_1$; 8) over-heating and destruction of the medium; 0) need to increase Δ, p, and η to compensate for the losses; 0*) need to increase the pump intensity. The letters represent countermeasures (Secs. 2–6): a) anomalous dilution; b) generalized two-stage pumping with transfer of the R^* nuclei; c) rf (or optical) pulse separation; d) fast resonant switches; e) traveling pump zone.

$s_0 \lesssim 1.05$. Each inversion $\eta > \eta_m$, where η_m is the minimum of $\eta_c(p,\xi)$ for a given ξ, corresponds to the minimum gain $p_e(\eta,\xi)$. Thus, allowance for superradiance, decay, and superluminescence yields the threshold conditions for "strong" (stable) lasing, which develops freely at times $t > t_p$, in spite of the fact that the pumping has stopped at t_p:

$$\eta \gtrsim \eta_m, \qquad p \gtrsim p_e(\eta,\xi) \equiv p_e, \qquad (5)$$

in contrast to "weak" (unstable) lasing comparable with noise, violating the condition (5), and possible only if the decay Δ is compensated by simultaneous pumping. Since $\Sigma' \approx 2n\sigma \approx 2n'\sigma'$ for dilution $n/n' \approx \sigma'/\sigma$, which is needed to cool the filament,[6] we can see that Eq. (5) leads to the following restrictions:

$$\Delta \gtrsim (1+wG)n_e\eta_m, \quad \Delta \gtrsim \Delta_0 \equiv 2p_e n'\sigma'/\sigma_0 = 2p_e n\sigma/\sigma_0, \qquad (6)$$

$$n_e \gtrsim 2p_e n'\sigma'/\eta_e(1+wG)\sigma_0, \quad p_e \ll \sigma_0/2\sigma \equiv p_m. \qquad (7)$$

Attainment of the threshold conditions is hindered also by overheating of the active medium (δT or J) which is not less than the contribution of conversion (δT_e or J_e). In the case of short-lived nuclei ($\tau_1 < 10^{-5}$ sec) such overheating is

$$\delta T \gtrsim \delta T_e \approx \frac{\varkappa n_e}{1+\alpha}\frac{E_\tau}{c_V} \gtrsim \frac{2p\alpha}{1+\alpha}\frac{E_\tau}{3\varkappa}\frac{\sigma'}{\sigma_0} > 10^3\ {}^\circ\text{K} \qquad (8)$$

($\varkappa$ is the Boltzmann constant), which is higher than the Debye temperature $T_D \lesssim 10^3\,^\circ\text{K}$ and, therefore, reduces $p \sim \sigma_0 \sim f$ to zero. In the case of long-lived nuclei the overheating flux across the surface

$$J \gtrsim J_e \gtrsim \frac{d}{4}\frac{2p\alpha}{1+\alpha}\frac{E_\tau}{\tau_1}\frac{\sigma'}{\sigma_0}n' > 10\quad\text{W/cm}^2 \qquad (9)$$

is greater than the flux $J_0 \approx 0.1$ W/cm² at which the necessary filament temperature $T \lesssim 1\,^\circ\text{K}$ (Ref. 4) is still possible.[17] Here, E_γ is the energy of the γ-ray transition, $c_v \approx 3\varkappa n'$ is the specific heat, $\varkappa = 8.6\times10^{-8}$ keV/$^\circ$K, and since for $d \ll 10^{-2}$ cm the γ-ray losses across the filament surface are strong,[16] we shall assume that $d \approx 10^{-2}$ cm, which exceeds the conversion electron range.

Thus, overheating is not reached to T_D and J_0 by the dilution $n/n' \approx \sigma'/\sigma$ and by the reduction of d, and it destroys the active medium in all types of γ-ray laser,[1-11] making lasing impossible. Overheating by the output radiation is less dangerous but it limits the output energy $\mathscr{E}$ per pulse (for pulses of $\tau_1 < 10^{-5}$ sec duration) or the power $\mathscr{P}$ (for $\tau_1 > 10^{-5}$ sec) of a γ-ray laser:

$$\mathscr{E} \lesssim c_V T_D L_0 \approx 3\cdot10^3\ \text{J/cm}^2\ , \quad \mathscr{P} \lesssim \frac{4L_0 J_0}{d} \approx 30\ \text{W/cm}^2\ . \qquad (10)$$

Heating, overheating, and other obstacles to γ-ray lasing enhance one another forming a single "complex of lasing obstacles" (Fig. 2). We shall now consider measures which can be taken against these obstacles.

2. ANOMALOUS DILUTION

We shall consider a filamentary crystal consisting of light atoms R' and we shall assume that the reflecting planes of this crystal $R'R'$ are parallel to the filament. We shall postulate that $d \gtrsim 10^{-2}$ cm, so that γ rays from R impurity nuclei feed a Borrmann mode (B mode) along the filament with a minimum of the amplitude A'_b in the $R'R'$ planes and a maximum A_b between the planes. If A_0 is the amplitude of an ordinary wave, in the case of a B mode we have

$$|A'_b|^2 = k'_b|A_0|^2, \quad |A_b|^2 = k_b|A_0|^2, \quad k'_b \ll k_b, \qquad (11)$$

where $k'_b \approx 10^{-2}$ and $k_b \approx 4$, i.e., a B wave passes through layers between the $R'R'$ planes.[18] Stronger anomalies characterized by $k'_b \lesssim 10^{-3}$ are not excluded. According to Andreev,[16] lasing occurs in a B mode. In approximate estimates we can adopt the opposite approach and assume that the wave is homogeneous but the cross sections are inhomogeneous: we can replace σ' for the R' atoms with $\sigma'k'_b$, and σ and σ_0 for the R atoms in the $R'R'$ planes (with a probability a') with $\sigma k'_b$ and $\sigma_0 k'_b$, and also replace σ and σ_0 for the R atoms between the $R'R'$ planes (with a probability $a = 1 - a'$) with σk_b and $\sigma_0 k_b$. In Eqs. (5)–(7) we replace n, n_e, Δ, μ_0, Σ', L_0, and p with

$$n_b \approx \tfrac{1}{2}nk_b', \quad n_{eb} \approx \tfrac{1}{2}n_ek_b', \quad \Delta_b \approx \tfrac{1}{2}\Delta k_b',$$

$$\mu_{0b} = \sigma_0(ak_b + a'k_b')\Delta_b \approx 2\sigma_0\Delta_b, \quad \Sigma_b' = \sigma(ak_b + a'k_b')n_b$$

$$+ \sigma'k_b'n' \approx k_b'\Sigma', \quad L_{0b} = 1/\Sigma_b' \approx L_0/k_b', \quad p_b = \mu_{0b}L_{0b} \approx \mu_0 L_0 = p \qquad (12)$$

and also replace the dilution condition $\sigma n \approx \sigma'n'$ with

$\sigma a k_b n_b \approx \sigma' k'_b n'$, where $a \approx \frac{1}{2}$ and $k_b \approx 4$. After these replacements Eqs. (6)–(10) become

$$\Delta_b \gtrless p_c n' k_b' \sigma'/\sigma_0, \quad n_b/n' \approx k_b '\sigma'/2\sigma \lesssim 10^{-4}-10^{-5}, \quad (13)$$

$$\delta T_{eb} \approx {}^1\!/_2 k_b' \delta T_e \lesssim 10-10^{2\,\circ}\text{K} \quad J_{eb} \approx \tfrac{1}{2} k_b 'J_e \lesssim 0,1 \text{ W/cm}^2, \quad (14)$$

$$\mathscr{E}_b \approx \mathscr{E}/k_b' \approx 3\cdot 10^5 \text{ J/cm}^2, \quad \mathscr{P}_b \approx \mathscr{P}/k_b' \approx 3\cdot 10^3 \text{ W/cm}^3. \quad (15)$$

According to Eq. (12), $\Delta/n = (\Delta/n)_b$. Therefore, there is no change in the pumping rate, which depends (see Sec. 3a) only on Δ/n. This means that the change to anomalous dilution in a B mode, i.e., the change from $n/n' = \sigma'/\sigma \approx 10^{-2}-10^{-3}$ to $n_b/n' \approx 10^{-4}-10^{-5}$ does not require an increase in the pumping rate so that the gain achieved remains $p = p_b$, and it makes possible: 1) the use of overheating to acceptable values given by Eq. (14); 2) increase the output values of $\mathscr{E}$ and $\mathscr{P}$; 3) increase L_0, and reduce d/L and the Fresnel number by a factor of k_b'; 4) facilitate line narrowing (see Sec. 4c); 5) reduce by a factor of 10^3-10^4 the superluminescence noise which develops only in B modes because in the other modes the absorption is characterized by $\mu_{abs} \approx \sigma' n' - \sigma_0 \Delta_b \gtrsim 0.5 \text{ cm}^{-1}$. Then, for $L = \xi L_{0b}$ the superluminescent acceleration of decay in the anomalous dilution case s_{AD} [see Eq. (2)] becomes

$$s_{AD} \approx 1 + \frac{B}{\pi^2} f_\alpha \frac{k_b'}{\xi} \frac{d}{L_0} \frac{e^{\mu L}}{\mu L}\left(1+\frac{2}{\mu L}\right), \quad B = \cos\vartheta\,\delta\vartheta \approx 10^{-3}, \quad (16)$$

where $\mu L = \xi(p-1) \gg 1$; ϑ and $\delta\vartheta$ are the Bragg angle and its half-width. Substitution of s_{aD} in place of s_0 in Eqs. (3) makes the minimum of $\eta_e(p)$ deeper (Fig. 1).

A. Attainment fo spin temperature $T_s \lesssim 0.01\,°$K in anomalous dilution method

In some γ-ray laser schemes one requires a low spin temperature of nuclei $T_s \lesssim 0.01°$K. For example, in the two-stage pumping system[8] (Fig. 3a) one should have $n_{g'} \lesssim 0.1\Delta_0$ so that $\Delta = n_e - n_{g'} > \Delta_0$ in the case of the e–g' laser transition. If

$$n_{g'} \approx nA^{-1}\exp(-E_{g'}/\varkappa T_s) \lesssim {}^1\!/_{10}\Delta,$$

where A is the partition function of the Zeeman sublevels and $E_{g'}$ is the energy of the hyperfine structure of the sublevel $|g'\rangle$, we find from Eq. (6) that

$$T_s \lesssim |(m'\pm j)gH_e\mu/\varkappa|/\ln(\sigma_0/\sigma) \approx 10^{-2}-10^{-3\,\circ}\text{K}, \quad (17)$$

where μ is the nuclear magneton; $\mu/\varkappa \approx 3.7 \times 10^{-8}\,°$K/Oe; $\pm j \equiv j \,\text{sign}(\mu gH_e)$; $j = j_g$ and $g = g_g$ are the spin and the g factor of the ground state of a nucleus R; m' is the projection of the spin on j; H_e is the effective magnetic field at a nucleus R; $H_e \approx 10^6 - 5\times 10^6$ Oe for magnetic ions and $H_e \approx 10^5$ Oe for nonmagnetic R ions located near magnetic ones; $T_s \lesssim 10^{-2}- 10^{-3}°$K is attainable[17] just before pumping begins.

If pumping heats the lattice to $T \gtrsim \delta T_e \gg T_s$, the spin-lattice relation is accelerated and it populates the sublevel $|g'\rangle$ by an amount $\delta n_{g'}$ at $t_p \gtrsim 2\tau_1$. It follows from $\delta n_{g'} \lesssim 0.1\Delta$ and from Eq. (6) that if the relaxation time is τ_s then

$$\delta n_{g'} \gtrsim \frac{2\tau_1}{\tau_s}\frac{n}{2j+1} \quad \tau_s \gtrsim \frac{\tau_1}{2j+1}\frac{\sigma_0}{\sigma}\frac{10}{p_e} \approx 10^3\tau_1 \gtrsim 10^{-2}-10^{-4} \text{ sec.} \quad (18)$$

However, the temperature given by Eq. (17) can be achieved only if $H_e \gtrsim 10^5 - 10^6$ Oe, i.e., when a nucleus
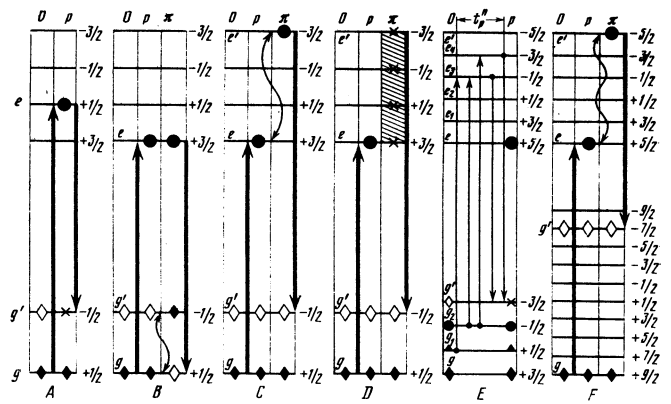

FIG. 3. Inversion schemes utilizing split hyperfine structure: A) fluorescence; B), C), D) main types of rf pulse separation schemes; F) modification of these schemes; E) nonselective activation. The shading represents mixing of sublevels. The points ◆, ▲, ●, ×, and ◇ represent populations in decreasing order. The various phases are denoted as follows: 0) initial; p) activation; π) inversion. In fluorescence schemes the phases p and π are not separated. Long-wavelength (for example, optical) models of rf pulse separation produce similar effects (Sec. 7).

R is located alongside or inside a paramagnetic center so that $\tau_s \approx \tau_{el}$ (Ref. 19), where τ_{el} is the electron spin relaxation time. According to Ref. 20, $\tau_{el} \gtrsim 10^{-2}-10^{-4}$ sec [see Eq. (18)] only at temperatures $T \lesssim 10-10^2°$K, which can be achieved solely in the anomalous dilution case.

In the following investigation of the feasibility of relaxing the pump conditions we shall combine the known methods[4,7,8,10,21] within the framework of an extended generalized two-stage pumping (GTSP) model so as to cover all types of γ transitions (long- and short-lived with a hyperfine structure and without it) and all types of activating fluxes: excited nuclei R^* (Refs. 6, 7, and 21), neutrons,[6,8] γ rays,[9,22] electrons,[23] etc.

3. FIRST STAGE OF GENERALIZED TWO-STAGE PUMPING AND ITS QUANTUM EFFICIENCY

As in the case of two-stage pumping, the source of resonant pumping M_1 in GTSP is spatially separate from the active medium (filament) M_2. This makes it easier to provide radiation protection of M_2 and to cool the target M_1 (if M_1 is a fine-dispersion medium with grains of $d_1 \lesssim 10^{-6}$ cm size, suspended in a cooling agent such as ^{4}He or deposited on a cooled substrate with fine pores) to $T \lesssim 10^2$ °K in the case of short-lived nuclei and to $T \lesssim 1$ °K in the case of long-lived nuclei. The disordered orientations and imperfections of crystallites in M_1 are unimportant in GTSP.

We shall assume that M_1 is a film of thickness h and that "quanta" of the primary activating flux Φ_0 (excited nuclei R^*, γ rays, electrons, neutrons, etc.) entered through the left-hand (entry) plane, whereas the right-hand (exit) plane is crossed in the direction of the target M_2 by a flux of resonant γ rays $\Phi_{\gamma 0}$. This is the transmission geometry. In the reflection geometry the left-hand plane of M_1 combines the role of the entry

for Φ_0 and exit for $\Phi_{\lambda 0}$.

The primary flux decreases with the depth x in M_1 in accordance with the law

$$\Phi(z) \approx \Phi_0 e^{-iz}, \qquad (19)$$

where Σ is the macroscopic cross section for the losses of Φ. In the case of the γ-ray flux Φ_λ the macroscopic loss cross section is

$$\Sigma_T = \sigma_{ei}(Gn_g - n_e) + \sigma_1 n_1 + \sigma_1' n_1' + \sigma_1'' n_1'', \qquad (20)$$

where n_1'', n_1', and n_1 are the concentrations of the nuclei R'' of the cooling agent (n_1''), of the nuclei R' in the grains (n_1'), and of the heavy nuclei (n_1), i.e., of the original nuclei R_0 and the active nuclei considered together; σ_{el}, σ_1, σ_1', and σ_1'' are the cross sections for the e–g resonant transition and for the nonresonant losses due to the atoms R_0, R, R', and R''. The concentrations and macroscopic cross sections are averaged over the heterogeneous medium M_1. It follows from Eqs. (19) and (20) that

$$n_e(z) \approx n_e(0) e^{-iz}, \quad \Sigma_T(z) \approx a e^{-iz} + b, \qquad (21)$$

where $n_e(0)$, a, and b are independent of z and give the following equation for the rise of Φ_γ:

$$\pm \frac{\partial}{\partial z} \Phi_T \approx r_1 n_e(z) - \Phi_T \Sigma_T(z), \quad r_1 = f_1 \frac{\delta \Omega}{4\pi \tau_1 (1 + \alpha_1)}, \qquad (22)$$

where f_1 and α_1 are the factors f and α [see Eq. (2)] for M_1; $\delta\Omega$ is the average (over M_1) solid angle used in the activation of M_2. The signs $\pm$ in Eq. (22) correspond to Φ_γ^+ in the transmission geometry and to Φ_γ^- in the reflection geometry. It follows from Eqs. (22) and (21) that

$$\Phi_T^+(z) = r_1 n_e(0) e^{i\alpha} \xi^\beta \int_\xi^1 u^{-\beta} e^{-\alpha u} \frac{du}{\Sigma}, \quad \xi = e^{-iz}, \quad \alpha = \frac{a}{\Sigma}, \qquad (23)$$

$$\Phi_T^-(z) = r_1 n_e(0) e^{-i\alpha} \xi^{-\beta} \int_{\xi_0}^1 u^\beta e^{\alpha u} \frac{du}{\Sigma}, \quad \xi_0 = e^{-hz}, \quad \beta = \frac{b}{\Sigma}.$$

Since ξ, $\xi_0 < 1$, $\alpha \ll 1$ [see Eqs. (26)–(28)], we find that at the exit from M_1

$$\Phi_T^+(h) \approx \Phi_{T0}^+ \approx r_1 n_e(0) [e^{-hb} - e^{-hz}]/(\Sigma - b),$$

$$\Phi_T^-(0) \approx \Phi_{T0}^- \approx r_1 n_e(0) [1 - e^{-h(z+b)}]/(\Sigma + b). \qquad (24)$$

The flux $\Phi_{\gamma 0}^+$ is maximal at $h = h_0$, whereas $\Phi_{\gamma 0}^-$ saturates in the limit $h \to \infty$, i.e.,

$$\Phi_{T0}^\pm \lesssim \sup \Phi_{T0}^\pm \approx r_1 n_e(0) y^\pm/\Sigma, \quad h_0 = \ln(\Sigma/b)/(\Sigma - b),$$

$$y^+ = \exp(\beta \ln \beta/(1 - \beta)), \quad y^- = 1/(1 + \beta) \gtrsim y^+ \approx 0.7 y^-. \qquad (25)$$

Let us assume that $\Phi_0 = \text{const}$ during the time interval $0 \le t \le t_p$. The values of Φ, Φ_γ, Σ, n_e, a, b, etc. for each specific type of activation will be denoted by a tilde (transfer of excited nuclei R^*), a bar (neutrons), or an asterisk (γ rays, Coulomb excitation). Allowing for the trapping levels $|h\rangle$, whose lifetime (compared with τ_1) is assumed to be infinite in model estimates, we find the parameters in Eq. (21), using the fact that they are independent of z, by solving the transport equations at $z = 0$.

If $\tilde\Phi_0$ is the flux of excited nuclei R^*, then

$$\tilde a = [G(1 - \tilde w_h)\sigma_{ei} + \sigma_1]\tilde n_1 - (G+1)\bar n_e(0)\sigma_{ei} \ll \tilde\Sigma,$$

$$\tilde b = \sigma' n_1' + \sigma'' n_1'', \quad \tilde n_1 = \tilde n_e + \tilde n_g + \tilde n_h = t\tilde\Phi_0\tilde\Sigma, \quad \tilde w_e + \tilde w_g + \tilde w_h = 1, \qquad (26)$$

$$\tilde n_e(0) = \tilde w_e \tau_1 \varphi_1(t/\tau_1)\tilde\Phi_0\tilde\Sigma, \quad \varphi_1(u) = 1 - e^{-u}.$$

It is assumed here that the beam losses $\tilde\Phi$ are due to implantation (precipitation) of the beam particles in a grain; allowance is made for the decay of the levels $|e_*\rangle$, $|e\rangle$ and for the distributions $\tilde w_e$, $\tilde w_s$, and $\tilde w_h$ of the R nuclei between $|e\rangle$, $|g\rangle$, and $|h\rangle$ in the beam $\tilde\Phi_0$.

If $\bar\Phi_0$ is a flux of particles which alter the composition of a nucleus (neutrons), then

$$\bar a \approx [G(1 - \bar w_h)t\bar\Phi_0\bar\Sigma - (G+1)\bar n_e(0)]\sigma_{ei} \ll \bar\Sigma,$$

$$\bar b \approx \sigma_1\bar n_{00} + \sigma' n_1' + \sigma'' n_1'', \quad \bar n_1 = \bar n_e + \bar n_g + \bar n_h + \bar n_0 = \bar n_{00} = \text{const}, \qquad (27)$$

$$\bar n_e(0) = \bar w_e \tau_1 \varphi_1(t/\tau_1)\bar\Phi_0\bar\Sigma, \quad \bar\Sigma \approx \sigma_T \bar n_0 \approx \sigma_T \bar n_{00},$$

where $\sigma_T \equiv \sigma_{n\gamma}(E_T)$ is the cross section of the $n\gamma$ capture in a case when the thermal neutron energy is $E_T = 0.026$ eV (and the thermal neutron velocity is $v_T = 2.24 \times 10^5$ cm/sec); $\bar\Phi_0 = \bar N_0 v_T$; $\bar N_0$ is the density of neutrons with an energy distribution $\bar N(E)$: $\bar N_0 = \int \bar N(E)dE$; $\bar n_{00}$, $\bar n_0 \equiv \bar n_0(t)$ are the initial and actual concentrations of the original nuclei R_0 transformed by the $n\gamma$ capture to the highly excited states $|e_*\rangle$ that decay to $|e\rangle$, $|g\rangle$, and $|h\rangle$ with the branching ratios $\bar w_e$, $\bar w_g$, and $\bar w_h$ obeying $\bar w_e + \bar w_g + \bar w_h = 1$. It is assumed that the losses of the beam $\bar\Phi$ are entirely due to the useful $n\gamma$ capture and that $\bar\Phi_0\sigma_T\tau_1 < 1$.

If Φ_0^* is a Coulomb excitation or a γ-ray flux, then

$$a^* \approx -\gamma^*\sigma_{ei}Gw_h^*t\Phi_0^*\Sigma^* - \sigma_{ei}n_e^*(0), \quad |a^*| \ll \Sigma^*,$$

$$b^* \approx n_1^*(G\sigma_{ei} + \sigma_1) + \sigma' n_1' + \sigma'' n_1'', \quad \gamma^* \lesssim \Sigma_e^*/\Gamma^*\tau_1^*\Sigma^* \ll 10^{-4}, \qquad (28)$$

$$n_e^*(0) \approx \gamma^* w_e^* \tau_1 \varphi_1(t/\tau_1)\Phi_0^*\Sigma^*, \quad w_e^* + w_g^* + w_h^* = 1,$$

where γ^* is the efficiency of excitation of the higher $|e_*\rangle$ levels; $\tau_1^* \gtrsim 10^{-12}$ sec is the lifetime of $|e_*\rangle$; $\Gamma^* \gtrsim 10^{15}$ sec^{-1} is the spectral width of the flux Φ^*; Σ_e^* is the resonant macroscopic cross section of the $g - e_*$ transition; Σ^* is the macroscopic cross section for all the losses of Φ^*; $\Sigma^* \gg \Sigma_e^*$; the condition $\gamma^*\tau_1\Sigma^*\Phi_0^* \ll n_1^*$; is always satisfied; w_e^*, w_g^*, and w_h^* are the branching factors for the transitions from $|e_*\rangle$ to $|e\rangle$, $|g\rangle$, and $|h\rangle$. Equations (25)–(28) yield the same type of formula for the optimal, in respect of h, quantum efficiency $q_1(t)$ of the resonant luminescence from M_1 entering M_2:

$$q_1(t) = \sup \frac{\Phi_{T0}^\pm}{\Phi_0} = \gamma w_e f_1 \varphi_1\left(\frac{t}{\tau_1}\right) y^\pm(\beta) \frac{\delta\Omega_2}{4\pi(1 + \alpha_1)}, \qquad (29)$$

where γ represents a generalization of γ^* from Eq. (28). In Eqs. (26) and (27), we have $\gamma \approx 1$. In contrast to $\delta\Omega$ in Eq. (22), the vertex of the solid angle $\delta\Omega_2$ is inside M_2. If M_2 is located coaxially inside a hollow cylinder M_1, then $\delta\Omega_2 \approx 4\pi$. If $t \gtrsim 2\tau_1$, then $\varphi_1(t/\tau_1) \approx 1$. The quantum efficiency q_1 can then reach the following values:

1) for activation with transfer of excited nuclei, as discussed, for example, in Refs. 6, 7, and 21,

$$\tilde q_1 \approx f_1/(1 + \alpha_1) \approx 0.1 - 0.01, \qquad (30)$$

since $\tilde\Sigma^{-1} \lesssim 10^{-4}$ cm (the range of R^* in a solid); $\tilde b^{-1} > 5$ cm, $\tilde\beta \lesssim 10^{-4}$, $\tilde y^\pm \approx 1_1$ 1, $\tilde w_e \approx 1$, if the excitation of nuclei[6,21] is combined with separation of the $|e\rangle$ state;[7]

2) for activation accompanied by a change in the com-

position of nuclei, as discussed for example in Refs. 6 and 8,

$$\bar{q}_1 \approx \bar{w}_e y^{\pm}(\beta)\, \tilde{q}_1 \approx 0.5 \tilde{q}_1 \sigma_T/(\sigma_1+\sigma_T) \approx 10^{-3}-10^{-5}, \qquad (31)$$

since $w_e \approx 0.5$, $\bar{\beta} \approx \sigma_1/\sigma_T \gtrsim 10^2 - 10^4$, and $y^{\pm}(\bar{\beta}) \lesssim 10^{-2}- 10^{-4}$ (Table I);

3) for activation by Coulomb photon excitation,[9,22,23]

$$q_1^* \approx \gamma^* w_e^* \tilde{q}_1 \ll 10^{-5}, \qquad (32)$$

since $\gamma^* \ll 10^{-4}$ and $\beta^* \approx n^* \sigma_e /\Sigma^* \approx \Sigma_e^*/\Sigma^* \ll 1$. Since $\tilde{q}_1 \gg \bar{q}_1 \gg q_1^*$, the process of activation involving the transfer of R^* nuclei[6,7,21] is to be preferred.

Our target M_1 is thus a converter of a wide-band flux of a generalized quanta Φ_0 entering the target into a flux of resonant luminescence $\Phi_{\gamma 0}$ at the exit. The converter is more stable against radiation than the filament M_2 and the quantum efficiency of the converter may reach $q_1 \approx 0.1$.

A. Second stage of generalized two-stage pumping. Realistic activation fluxes

In the second stage of GTSP which occurs in the target M_2, it is very convenient to use schemes[8] called here fluorescence schemes (Fig. 3A), since a flux $\Phi_{\gamma 0}$ of frequency ω populates the level $|e\rangle$ and the active transition e-g' of frequency ω' terminates at an initially empty lower level $|g'\rangle$. Let us assume that $\Phi_{\gamma 0}=0$ and $n_e = n_{g'} = 0$ at $t < 0$, but $\Phi_{\gamma 0} = \text{const} > 0$ at $t \geq 0$ (instantaneous change). The large-signal approximation with $n_e \ll n_g$ gives (see Sec. 3.132 in Ref. 24)

$$n_e(t) = n_\infty \varphi_1^2(u/2), \quad n_\infty = n_g \Phi_{\gamma 0}\sigma_{eg}\Gamma_1^{-1}, \quad u = t/\tau_1, \qquad (33)$$

$$\Delta(t) = n_e(t) - n_{g'}(t) = n_\infty\{(1+w)\varphi_1^2(u/2) + w[2\varphi_1(u/2) - u]\}, \qquad (34)$$

where Γ_1 is the spectral width of $\Phi_{\gamma 0}$; σ_{eg} is the averaged (over the polarization and angles) cross section of the e-g transition; w is the branching ratio of the e-g' decay.

If during the pump time t_p a maximum of Δ is reached [see Eq. (1)], then

$$t_p/\tau_1 = u_m = 2\ln(1+w^{-1}), \quad \Delta_m \equiv \Delta = n_\infty \delta_m, \quad n_{em} \equiv n_e = n_\infty(1+w)^{-2}, \qquad (35)$$

where

$$\delta_m = \eta(1+w)^{-1}, \quad \eta = 1+2w - w(w+1)u_m = \Delta/((1+w)n_e). \qquad (36)$$

Since $\sigma_{eg}\sigma_0 \lesssim (1-w)w\varkappa_0\sigma_e^2$, where σ_e is the resonant cross section in the absence of a hyperfine structure, $\varkappa_0 = \sigma_0/\sigma_{eg'} \lesssim l+\frac{1}{2}$, and l is the multipolarity of a γ transition, it follows from Eqs. (33), (35), and (6) that a resonant flux used during the pump time t_p has the form

$$F_{20} = t_p \Phi_{\gamma 0} = t_p \Gamma_1 \Delta/\delta_m n_g \sigma_{eg} \gtrsim 200 p_e y_s \tau_1 \Gamma_1 F_e, \quad F_e = \sigma/\varkappa_0\sigma_e^2, \qquad (37)$$

where $y_s = 0.01 u_m/u(1-w)\delta_m$. The correspondence between $\eta_e(p)$ (Fig. 1) and $\eta(w)$ (Fig. 4) gives $p_e(w)$ and a curve $F_{20}(w)/F_e$ (Fig. 5) with a minimum, which yields for $\xi = 1$ the following values optimal in the case of fluorescence systems:

$$w \approx 0.26, \quad \delta_m \approx 0.38, \quad p_e \approx 7.8, \quad \eta_e \approx 0.48, \quad t_p \approx 3.1\tau_1, \qquad (38)$$

$$F_{20} \approx 650 F_e \gtrsim 10^{18}\ \text{cm}^{-2}. \qquad (39)$$

Since at $t \lesssim t_p$ the population inversion Δ is lost by

TABLE I. Table of some lasing γ-ray transitions.

No.	Eq. No.	Parameters	⁴⁰K	⁵⁷Fe	⁸³Kr	¹⁶¹Dy	¹⁸¹Ta	¹⁰⁹Ag
1	(9)	E_γ, keV	29.56	14.41	9.35	25.66	6.23	88.0
2	(1)	τ_1, sec	6.2(-9)	1.4(-7)	2.1(-7)	4.1(-8)	9.8(-6)	57.4
3	(37)	σ_e, bn	2.4(5)	1.2(6)	1.4(6)	8.1(5)	1.3(6)	3.0(3)
4	(1)	σ, bn	2.3(2)	5.7(3)	8.6(3)	6.6(3)	9.2(4)	3.7(2)
5	(1)	σ', bn	2.7	4.8	11.0	2.0	36.0	2.1
6	(27)	σ_T, bn	2.0	2.7	45.0	61.0	700.0	?
7	(2)	α	6.6	8.2	17.9	2.9	46.0	9.4
8	(1)	G	0.78	2	0.8	1	1.25	4
9	(2)	f	0.65	0.92	0.97	0.85	0.99	0.10
10	(1)	L_0, cm	1.5	0.9	0.37	1.4	0.12	2.0
11	(6)	n/n'	1.2(-2)	8.4(-4)	1.3(-3)	4.4(-4)	3.9(-4)	5.6(-3)
12	(8)	δT_e, °K	1.5(4)	2.7(3)	3.6(3)	2.4(3)	1.7(3)	
13	(6),(1)	Δ/p, cm⁻³	1.8(18)	6.5(17)	1.3(18)	5.7(17)	4.3(18)	4.9(19)
14	(6),(1)	Δ/np	1.3(-3)	6.3(-3)	8.2(-3)	1.1(-2)	9.4(-2)	7.0(-2)
15	(37)	F_e, cm⁻²	2.7(15)	2.7(15)	2.9(15)	6.7(15)	3.6(16)	1.2(19)
16	(38),(2),(35)	t_p, sec	1.9(-8)	4.3(-7)	6.5(-7)	1.4(-7)	3.0(-5)	178
17	(40)	F_{2r}, cm⁻²	1.8(19)	1.8(19)	1.9(19)	4.4(19)	2.3(20)	7.8(22)
18	(31)	$\bar{q}_1$	3.7(-4)	2.1(-5)	1.3(-4)	1.0(-3)	7.9(-5)	?
19	(41)	F_{1r}, cm⁻²	4.8(22)	8.4(23)	1.5(23)	4.4(22)	2.9(24)	?
20	(27),(41)	$\bar{N}_{0r}$, cm⁻³	1.1(25)	8.7(24)	1.0(24)	1.4(24)	4.3(23)	?
21	(30)	$\tilde{q}$	8.6(-2)	0.1	0.05	0.22	2.1(-2)	9.6(-3)
22	(41)	$\tilde{F}_{1r}$, cm⁻²	2.1(20)	1.8(20)	3.7(20)	2.0(20)	1.1(22)	8.1(24)
23	(62)	$F_e E_\gamma$, J/cm²	1.3(4)	1.3(3)	0.7(3)	3.4(3)	0.5(3)	1.3(6)
24	(43)	t_p'', sec	1.6(-8)	3.5(-7)	5.3(-7)	1.0(-7)	2.5(-5)	144
25	(63)	F^*_{2a}, cm⁻²	2.7(16)	2.7(16)	2.9(16)	6.7(16)	3.6(17)	1.2(20)
26	(27),(63)	$\bar{N}''_{0a}$, cm⁻³	2.1(22)	1.7(22)	1.9(21)	2.6(21)	8.2(20)	?
72	(63)	$\bar{F}^*_{1a}$, cm⁻²	7.3(19)	1.3(21)	2.2(20)	6.7(19)	4.6(21)	?
28	(63)	$\tilde{F}^*_{1a}$, cm⁻²	3.2(17)	2.7(17)	5.7(17)	3.1(17)	1.7(19)	1.3(22)
29	(64)	$F^{(1)}$, cm⁻²	2.8(14)	0.9(14)	1.9(14)	0.9(14)	6.4(14)	1.7(16)
30	(64)	$F^{(1)}$, cm⁻²	2.6(21)	9.4(21)	7.2(20)	7.2(20)	5.4(20)	?
31	(27),(64)	$\bar{N}^{(1)}$, cm⁻³	7.5(23)	1.2(23)	6.2(21)	2.8(22)	9.6(19)	?
32	(64),(65)	$\delta T_s^{(1)}$, °K	145	525	40.3	40.3	30.3	?
33	(63),(65)	$\delta\bar{T}''_{sa}$, °K	4.1	72.8	12.3	3.8	258	?
34	(63),(65)	$\delta\tilde{T}_{sa}$, °K	129	2300	390	120	8200	?

Note. The transition constants are taken from Ref. 33. The notation 1.6(−8) or 7.3(19) denotes 1.6×10^{-8} or 7.3×10^{19}. The second column gives the number of the equation defining the parameter. For example, $\bar{N}''_{0a}$ is the density of thermal neutrons given by Eq. (27) corresponding to the flux $\bar{F}''_{1a}$, given by Eq. (63). The factor f is cited for 0 °K when $T_D \approx 3000 A^{-1/2}$°K, where A is the atomic number of a nucleus R. Here, $n' \approx 1.2\times10^{23}$ cm⁻³, $d \approx 10^{-2}$ cm, $\Gamma\tau_1 \approx 1$, $w \approx 0.5$, $\sigma_e \approx f_\alpha \lambda^2/\pi$, λ is the wavelength, and f_α is defined by Eq. (2). We have in all cases $\varkappa_0 = 1.5$, with the exception of ¹⁰⁹Ag, when $\varkappa_0 = 3.5$. There may be some disagreement between the values at the second decimal place because of rounding of numbers. A bar above a quantity represents neutron activation and a tilde represents implantation of the R^* nuclei (Sec. 3); the indices have the following meaning: (1) one-stage combined scheme (Sec. 6b); a) asymptotic γ-ray π pulse (Sec. 6); s) neutron scattering; p) pumping; r) allowance for losses in fluorescence schemes; 0) activating primary flux; subscripts 1 and 2 represent the targets M_1 or M_2 (Secs. 3 and 4); double prime (for example, t_p'') represents the use of rf or optical pulse separation methods. The cross sections for the stimulated excitation of a γ-ray transition are as follows: σ_0 is the cross section for a specific component of the hyperfine structure of the e—g transition in the case of a specific polarization and other parameters (for example, the wave vector) of the exciting wave; σ_{eg} is the same cross section as σ_0 but averaged over all the parameters of the exciting waves when they exhibit a scatter; σ_e is the effective cross section for the γ-ray transition as a whole, typical of unpolarized nuclei in the absence of a hyperfine structure. The rough agreement between the values of σ_0, σ_{eg}, and σ_e used in the derivation of Eq. (37) is sufficient for relative qualitative estimates of Eqs. (40), (41), (63), and (64).

In row 12, we have $p \approx 10$, with the exception of the Ta and Ag nuclei in which case we have to take $p \approx 2 \ll p_m \approx 10$ on the basis of Eq. (7). In rows 17, 19, 20, and 22, we have $p=7.8$. In row 23, we have $p \approx 2$ and the attainable energy fluxes are close to the maximum permissible [Eqs. (10) and (15)]. In rows 25–31, the corresponding values are $p \gtrsim 1$. $E = 1$ eV for rows 32 and 33. In row 34, $E = 10$ eV and this prevents polarization of M_1; $\delta\tilde{T}''_{sa}$ is the overheating due to the scattering of neutrons in the case of a two-stage combined scheme. In row 12, the heat flow across the filament surface for ¹⁰⁹Ag is $J_e \approx 54$ W/cm².

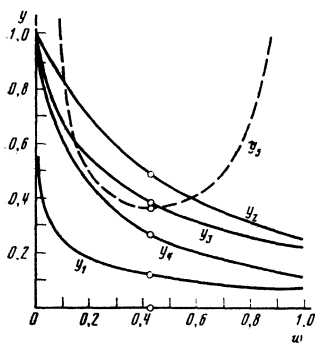FIG. 4. Dependences of the following quantities on w: $y_1 = 0.05 t_p / \tau_1$, $y_2 = n_e / n_\infty$, $y_3 = \eta$, $y_4 = \Delta / n_\infty$, and $y_5 = 0.01 u_m / \delta_m w (1 - w)$ for $G = 1$ in fluorescence schemes. The points are optima of Eqs. (38) and (39).

decay and weak lasing [see Eq. (5)], the estimates in Eqs. (37)–(39) should be increased by a factor of $k_{sg} = 1 + I_g / I_s \approx 1 + p\xi / 2 \approx 5$ where I_s and I_g are the rates of the usual decay and weak lasing found in Ref. 16. Allowing also for the influence of the inhomogeneity of the threshold conditions at $t \approx t_p$ by introducing the factor $k_u \approx 1.5$–2, we actually find that

$$F_{20}^{real} \equiv F_{2r} = k_{sg} k_u F_{20} \approx 10 F_{20} \gtrsim 6.5 \cdot 10^3 F_e \approx 10^{19} \text{ cm}^{-2}, \qquad (40)$$

and hence Eqs. (30)–(32) yield the following realistic primary activation fluxes

$$F_{1r} = F_{2r} / \bar{q}_1 \gtrsim 10^{20} \text{ cm}^{-2}, \quad \bar{F}_{1r} = F_{2r} / \bar{q}_1 \gtrsim 10^{22} \text{ cm}^{-2},$$
$$F_{1r}^* = F_{2r} / q_1^* \gg 10^{24} \text{ cm}^{-2}. \qquad (41)$$

B. Generalized two-stage pumping schemes with lower level decay

We can attempt to reduce the fluxes F_{20} and F_{10} by GTSP with the lower active level not the ground state but a short-lived level $|g_*\rangle$, exactly as in one-stage schemes.[7],[10] If we assume that $2\tau_1' \lesssim \tau_1$, where τ_1 and τ_1' are the lifetimes of the levels $|e\rangle$ and $|g_*\rangle$ of the active transition $e-g_*$, we find by analogy with Eq. (37) that the threshold resonant flux F_{20}' at the frequency of the inactive transition $e-g$ and the realistic pumping fluxes F_{2r}' and F_{1r}' are given by

$$F_{20}' \gtrsim 2 \cdot 10^3 F_e \approx 3 F_{20}, \quad F_{2r}' \gtrsim 3 F_{2r}, \quad F_{1r}' \gtrsim 3 F_{1r}. \qquad (42)$$
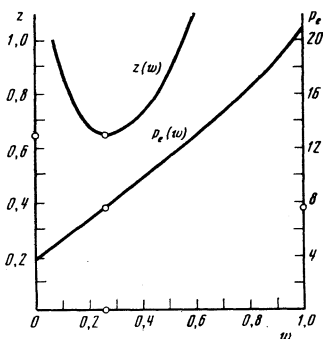
We can thus see GTSP schemes with decay of the lower

FIG. 5. Dependences, on w, of the amplification threshold $p_e(w)$ and resonant flux $z(w) = 10^{-3} F_{20} / F_e$ (on the scale of $10^3 F_e$) in fluorescence schemes with $\Gamma_1 \tau_1 \approx \xi \approx 1$ in the absence of losses. The points represent the minima of F_{20} with respect to w and p.

level do not relax the threshold conditions compared with fluorescence schemes of the types shown in Fig. 3A. We shall now describe schemes with much lower requirements in respect of the fluxes F_{2r} and F_{1r}.

4. PULSE SEPARATION OF ACTIVATION AND INVERSION PROCESSES IN GENERALIZED TWO-STAGE PUMPING

We shall begin by considering schemes for rf pulse separation of the processes of activation and population inversion in GTSP, similar to schemes employing multilevel fluorescence (Fig. 3A) decay of lower level, optical laser, gamma magnetic resonance (NMR + Mössbauer effect),[25] and ENDOR[20] methods.[2] Without any loss of generality, we shall consider three main types of rf pulse separation schemes (B, C, and D in Fig. 3) by discussing the example of a dipole $\frac{3}{2}$–$\frac{1}{2}$ transition in the case of the Zeeman hyperfine structure. Initially, at $t = 0$, the sublevel $|g\rangle$ is occupied (black rhomb) and the sublevel $|g'\rangle$ is empty (white rhomb). Selective activation $\Phi_{\gamma 0}$ is now applied (straight arrow pointing upward). After a time t_p'' the population of the sublevel $|e\rangle$ reaches its optimal value n_e (black circle) and the sublevel $|g'\rangle$ remains empty (white rhomb) since the $|\frac{3}{2}, \frac{3}{2}\rangle - |\frac{3}{2}, -\frac{1}{2}\rangle$ transition is forbidden. From the moment t_p'' the schemes B, C, and D of Fig. 3 begin to differ. We shall consider the scheme B in Fig. 3.

At the moment t_p'' the sublevels $|g\rangle$ and $|g'\rangle$ become inverted (wavy arrow) by an rf π pulse of duration $t_\pi \ll \tau_1$. Then, at the moment $t_{p\pi} = t_p'' + t_\pi$ we find that the sublevel $|g'\rangle$ is occupied and the sublevel $|g\rangle$ is empty. This implies an almost instantaneous appearance of 100% population inversion $\Delta = n_e$ of the active transition $e-g$. At this stage γ-ray lasing begins (downward arrow). Thus, we can consider a scheme of the type B to be divided (Fig. 3B) into an initial phase 0 at times $t \leq 0$, when $\Phi_\gamma = 0$ and $n_{g'} = 0$, an activation phase p when n_e increases but there is no population inversion since $n_g \gg n_e$, and an inversion phase π when the 100% population inversion $\Delta = n_e$ appears abruptly at $t = t_{p\pi}$.

A. Stability of C-Type schemes. Modification of rf pulse separation. Comparison with fluorescence schemes

Since π pulses are imperfect, a fraction $\zeta \gtrsim 10^{-2}$–10^{-4} of nuclei remains up to $t_{p\pi}$ at the original levels and instead of $\Delta = n_e$ we find that a realistic B-type scheme is characterized by $\Delta = n_e - \zeta n_g \ll n_e$ because $n_g \approx n \gg n_e$. This difficulty is avoided in C-type rf pulse separation schemes. At a moment t_p'' the upper sublevels $|e\rangle$ and $|e''\rangle$ are inverted (wavy arrow in Fig. 3C); then the population n_e accumulated at the level $|e\rangle$ is transferred at the moment $t_{p\pi}$ to the level $|e'\rangle$. Thus, the allowed $e'-g'$ transition creates instantaneously a population inversion $\Delta = n_{e'} \approx n_e$ and lasing begins with $\Delta / n_{e'} = 100\%$, exactly as in a perfect B-type scheme.

In addition to the B- and C-type schemes, one may also visualize simpler schemes of type D, where instead of a π pulse during the π phase (Fig. 3D) use is made either of a saturating rf pulse or of a φ pulse ($\varphi \neq \pi$). These D-type schemes mix the upper states $|e\rangle$ and

after a time $t_\pi \ll \tau_1$ they create an inversion $\Delta/n_{e'} = 100\%$ approaching for $j_e \lesssim 1$ the efficiencies of schemes B and C.

In view of the varied nature of the hyperfine structure of the R nuclei, we can have other modifications of the rf pulse separation schemes, for example a modification of a C-type scheme (F in Fig. 3) involving a quadrupole transition.

Schemes with rf pulse separation can ensure $w = 1$ in the pumping and lasing channels simultaneously so that we have $\sigma_{eg} = \sigma_0/\varkappa_0$ and $n_e = \Delta$ (or $n_{e'} = \Delta$), $\eta = 0.5$ and $p_e \approx 7.5$ for $\xi \approx 1$ (see Fig. 1). It then follows from Eq. (33) that a realistic flux is

$$F_{2r}'' = F_{20}'' = t_p'' \Phi_{10}'' = \frac{n_\infty \Gamma_1}{n_g \sigma_{eg}} t_p'' \geqslant \min_u \frac{2\Gamma_1 \tau_1 p_e \sigma u}{\sigma_{eg} \sigma_0 \varphi_1^2 (u/2)} \gtrsim 74 F_e, \quad (43)$$

since there is no inversion at times $t < t_b'' = 2.513\tau_1$ (see Fig. 3) and, therefore, there is no weak lasing or any inhomogeneity in the medium near the threshold giving rise to the factor $k_{sg} k_u$ in Eq. (40). We thus find that the rf pulse separation schemes require pumping fluxes which are $F_{2r}/F_{2r}'' \approx 88 \approx 10^2$ times less than those needed in simple fluorescence schemes (Fig. 3A). Since the superluminescence noise is suppressed ($s_0 \equiv 1$) in the rf pulse separation schemes, the dependences $\eta(p)$ (denoted by chain curves in Fig. 1) show a monotonic fall admitting in principle the possibility of exceeding the threshold with $p\xi \gg p_e\xi \approx 8$.

B. Long-lived isomers. Narrowing of hyperfine structure lines without external action

It is difficult to apply rf pulse separation in the case of long-lived isomers because of incompatibility of such separation schemes with rf line-narrowing methods.[5,16] However, we can use a different narrowing technique.

If the host matrix consists entirely of pure R' isotopes with a nuclear spin $j = 0$ (He^4, C^{12}, O^{16}, Ne^{20}, Mg^{24}, Si^{28}) and is diamagnetic, anomalous dilution suppresses magnetic-dipole broadening, which is 10^4–10^5 Hz in the absence of dilution,[4] by a factor of $(n/n')_b \approx 10^{-4}$–10^{-5}, i.e., the broadening becomes 1–0.1 Hz. Since in principle we can suppress the other causes of broadening by optical methods[26] or even without any external action,[4,27] our B and C schemes are suitable also in the case of long-lived isomers. This feature of anomalous dilution making possible hyperfine line narrowing without external action can be used also independently as a new method of γ-ray spectroscopy of long-lived isomers in which diamagnetic dilution of an absorber can be made lower than

$$(n/n')_\gamma \lesssim k_b' \sigma'/2\sigma_0 \approx 10^{-6} - 10^{-8}, \quad (44)$$

without loss of sensitivity and thus reduce the inhomogeneous dipole broadening to 10^{-2}–10^{-3} Hz. Suppression of other causes of broadening requires studies of the hyperfine structure of many-electron systems with a precision which has not yet been achieved.[27]

C. Conditions for implementation of rf pulse separation schemes

Decay in time t_π does not violate the threshold condi-

tions of Eq. (5) if

$$t_\pi \lesssim 0.05\tau_1 \ll t_0 + t_{lh} \approx \eta_e \tau_1 \approx 0.5\tau_1, \quad (45)$$

which sets limits on the amplitude H_{10}, carrier frequency of the rf field ν_0, and field H_e:

$$H_{10} = \pi H_0/2 g\gamma_n H_e t_\pi \approx 10^{-5}/g\tau_1 | \text{Oe} \cdot \text{sec} \approx 10 - 10^2 \text{Oe}, \quad (46)$$

$$\nu_0 \gtrsim 10/t_\pi \approx 10^2 - 10^3 \text{ MHz}, \quad H_e = 2\pi\nu_0/g\gamma_n \approx 10^5 - 10^6 \text{ Oe}. \quad (47)$$

For the B-type schemes we have $g = g_e$, whereas for the C-type schemes, we find that $g = g_e$; $H_e/H_0 \approx 10^3$ is the Fermi enhancement of the amplitude of the rf field at a nucleus by the contact Fermi field H_e (see Ref. 27, where the Fermi enhancement is shown to reduce line widths); $H_0 \approx 10^2$ Oe is a stabilizing external field. Overheating by a single π pulse is unimportant.[27] The conditions for rf pulse separation in respect of temperature, magnetic fields, spin-lattice relaxation (see Sec. 2a), an activation selectivity are the same as for the fluorescence schemes. Thus, if $n_{g'} \approx n_{g_2} \approx n_g$ (Fig. 3E) and the process is nonselective, the level $|g'\rangle$ becomes filled by the time t_b and the rf pulse separation does not operate. We can make the conditions (45)–(47) and (17) compatible if $\tau_1 \gtrsim 10^{-7}$ sec.

Difficulties limit the rf pulse separation method (see Secs. 4b and 4c) to the nuclei with $\tau_1 \approx 10^{-5}$–10^{-7} sec. The nuclei with $j = 0$ are completely unsuitable for this pulse separation method. Optical schemes proposed below do not require splitting of the hyperfine structure and extend the range of usable nuclei.

D. Optical pulse separation of activation and inversion in generalized two-stage pumping

Let us assume that there is no hyperfine structure. Activation of M_2 ensures filling of the unsplit level $|e\rangle$ and an optical π pulse applied at a moment t_p'' excites only $[R_e]$ ions (atoms) which have R nuclei in the excited state $|e\rangle$. The Mössbauer frequency ω^* of an R nucleus in an excited $[R_e]^*$ ion is displaced[26,27] relative to the frequency ω of the same nucleus R in an unexcited ion $[R]$. Therefore, ω^* is not absorbed (if $|\omega^* - \omega|\tau_2 > 1$) by the R nuclei which at the moment t_p'' are in the state $|g\rangle$ in the $[R]$ ions. Therefore at a moment $t_{p_\pi} = t_p'' + t_\pi^{0p} t$ we obtain 100% inversion $\Delta = n_e$ and thus achieve optical pulse separation of the activation, inversion, and lasing stages at the frequency ω^*.

The population inversion created in this way does not decay faster than according to Eq. (1) if the lifetime of the $[R_e]^*$ excited ions is $T_1^* \gtrsim \tau_1$. However, this restriction can be lifted by selective excitation in optical pulse separation with the aid of multilevel combined schemes of pulsed[26] or continuous[27] action designed specifically to increase effectively the electronic state lifetime of the $[R_e]^*$ ions to $t \gtrsim \tau_1$ without relaxation broadening of the hyperfine structure. These combined optical pulse separation schemes can also be applied to a wider (compared with rf pulse separation) range of nuclei with $\tau_1 \approx 10^{-2}$–10^{-9} sec.

We can regard optical pulse separation as a special kind of combined scheme. In fact, the combined schemes mix the ground $[R_e]$ and excited $[R_e]^*$ and $[R_e]^{*'}$ levels of the $[R]$ ion with a nucleus in the $|e\rangle$ state. On

S. V. Karyagin

transition of the nucleus to the lower state $|g\rangle$ these levels become the displaced levels $[R_e]$, $[R_e]^*$, and $[R_e]^{*\prime}$ which are not mixed by the action of a combined scheme and relax rapidly ($T_1^* \ll \tau_1$) to the state $[R_e]$ in which the γ-ray absorption frequency ω differs from the γ-ray stimulated emission frequency $\omega^* \neq \omega$. If $T_1^* \gtrsim \tau_1$, an optical π pulse should be followed by continuous combined mixing of the $[R_e]^*$ and $[R_e]^{*\prime}$ levels, which results in γ-ray absorption at a frequency $\omega^{*\prime} \neq \omega^*$ in some of the ions. We can see that in the case of optical pulse separation the frequencies of γ-ray emission ω^* and γ-ray absorption ω and $\omega^{*\prime}$ are different throughout the lasing process, exactly as in the case of excimer lasers, which reduces the threshold F_{2r}'' by a factor of 1.5–2 compared with the rf pulse separation. Similar action is produced by a variant of optical separation with π pulses involving the $[R_e] - [R_e]^*$ transition when the levels are subsequently mixed selectively by a combined scheme in order to maintain the difference between the γ-ray lasing frequency ω and the γ-ray absorption frequency $\omega^* \neq \omega$. In some cases the operation of an optical pulse separation scheme can be assured simply by a simplest combined scheme in the form of a saturating laser field.[27]

Selective excitation of $[R_e]$ atoms in a crystal can be produced by optical no-phonon (NP) lines of width $\Gamma_{NP} \approx 10^8 - 10^9$ sec^{-1} at temperatures $T \lesssim 10\,°$K if a shift $\delta\omega_{NP} \gtrsim 10^8 - 10^{10}$ sec^{-1} of such a line is possible as a result of a change in the state of a nucleus subject to the conditions $\Gamma_{NP} \lesssim 1/t_\pi^{opt} \ll \delta\omega_{NP}$ and $\Gamma_{NP}/\delta\omega_{NP} \lesssim (\sigma/\sigma_0)^{1/2}$. Optical pulse separation [see Eq. (45)] can be used if

$$\tau_1 \gtrsim 20 t_\pi^{opt} \gtrsim 20 (\delta\omega_{NP})^{-1} \approx 10^{-7} - 10^{-9} \text{ sec}, \tag{48}$$

i.e., it can be applied to practically all the Mössbauer nuclei including long-lived isomers, since optical pulse separation schemes are compatible with a line-narrowing rf field,[5] in contrast to rf pulse separation schemes.

Optical pulse separation is not affected by nonselectivity of γ activation or by imperfections of an optical π pulse. If $\Gamma_{NP} \approx 10^9$ sec^{-1}, $T_1^* \approx 10^{-4}$ sec, and $t_\pi^{opt} \approx 10^{-10} - 10^{-9}$ sec the energy of an optical π pulse can be less than 1–0.01 J cm^2 and no overheating results in the case of anomalous dilution. In contrast to the rf methods, optical pulse separation operates irrespective of hyperfine splitting, including the case when $j = 0$.

We can thus see that rf and optical pulse methods for separating activation, inversion, and lasing stages ensure that

$$\Delta/n_e = 100\%, \quad \eta \lesssim 0.5, \quad F_{2r}'' \lesssim 74 F_e \approx 10^{-2} F_{2r},$$

make certain that initial lasing conditions are homogeneous, suppress weak lasing and superluminescence noise, and make it possible to utilize many Mössbauer nuclei. Shutters discussed below ensure further relaxation of the pumping conditions.

5. FAST RESONANT SWITCHES

Absorbing resonant filters P with a large macroscopic absorption cross section Σ_{f0} can be used to divide an active filament M_2 of length L into m radiation-de-

coupled parts M_2' in such a way that in each of them the gain $\mu_0 L'$ does not create subthreshold losses for $p > 1$ (Fig. 2). A population inversion Δ_0 is created in each part M_2' after a time $t_{p\pi}$ by applying fluorescence, rf or optical separation schemes; then, after a time $\tau_F < t_\pi$ (ideally, $\tau_F = 0$) the filters P become bleached, i.e., the macroscopic absorption cross section Σ_F decreases ideally to zero. Then, from the moment $t_{pF} = t_{p\pi} + \tau_F$, lasing takes place throughout the length of the filament $L \gg L'$ and—because of the favorable initial conditions not spoiled by prethreshold perturbations and switching processes—such lasing should be homogeneous, stable, and characterized by lower losses than those in the case of the fluorescence or rf and optical pulse separation schemes when the condition (45) is not obeyed. If we assume that $\tau_F < t_\pi < 0.05\tau_1$ [see Eq. (45)], we find that $\tau_1 \approx 10^{-6} - 10^{-9}$ sec corresponds to

$$\tau_F \lesssim 0.01\tau_1 \approx 10^{-8} - 10^{-11} \text{ sec.} \tag{49}$$

However, the available mechanical and rf switches for γ-rays lasers[28] are characterized by insufficiently short switching times $\tau_F > 10^{-8}$ sec. We shall describe the principles of fast resonant switches with $\tau_F \approx 10^{-12}$ sec. Switches for short-lived nuclei are bleached by suppressing the Mössbauer spectrum as a result of overheating of a filter P to $T = T_F$ $T_D \approx 500\,°$K. Bleaching of fast resonant switches in the case of long-lived transitions requires simply overheating of a filter P by a fraction of a degree because then the temperature shift and violation of the Khokhlov condition $T \lesssim 1\,°$K (Ref. 4) take the filter off resonance. Bleaching can also be produced by optical excitation, since the R nuclei of excited $[R]^*$ atoms are off resonance. As in the case of optical lasers, bleaching by saturation of γ-ray absorption is possible only near a lasing peak at times $t \gtrsim t_p + t_0$.

In the case of an active fast resonant switch the heating is provided by an external source which may be an optical laser pulse or a current pulse. We shall assume that the nuclei R in such an active switch are in a crystallochemical environment (in a complex, molecule, or matrix) such that the frequency of the γ-ray lasing transition is absorbed resonantly by the R nuclei and the process is characterized by a macroscopic cross section $\Sigma_0 \approx 100$ cm^{-1} and nonresonant losses

$$\Sigma' \approx 1 \text{ cm}^{-1} \ll \Sigma_{F0} = \Sigma_0 + \Sigma' \approx 10^2 \text{ cm}^{-1}. \tag{50}$$

Let us assume that the body of such an active switch is a segment of a filament (cylinder) M_2 of length $L_F \approx 0.1$ cm screened from the pump radiation (see Sec. 5a below). At a moment $t_{p\pi}$ the lateral surface of the switch (of area $d \times L_F$) receives an optical laser pulse of duration $t_d \lesssim 10^{-12}$ sec. Uniform heating is ensured when the cylinder is optically semitransparent, i.e.,

$$d\Sigma_{opt} \lesssim 1, \tag{51}$$

where $\Sigma_{opt} \lesssim 100$ cm^{-1} is the optical absorption coefficient. A switch can be heated to the bleaching point T_F if the optical pulse energy is

$$Q_{opt} \gtrsim 2 \times 3 \varkappa T_F N_F \lesssim 0.03 \text{ J}, \tag{52}$$

where the factor $\gtrsim 2$ accounts for semitransparency;

$N_F = 10^{18}$ is the number of all the nuclei (R and R') in the switch; 0.03 J corresponds to $T_F \approx 500\,°K$.

We can thus see that under such conditions a fast resonant switch is bleached in $\tau_F \approx 10^{-12}$ sec. The transmission coefficients of an active switch in the nontransmitting ($k_\perp$) and transmitting ($k_\parallel$) positions are

$$k(t_{pn}) = k_\perp = \exp[-L_F(\Sigma_0 + \Sigma')] \lesssim 4 \cdot 10^{-5}, \tag{53}$$

$$k(t_{pn} + \tau_0) = k_\parallel = \exp(-L_F \Sigma') \gtrsim 0.90. \tag{54}$$

A. Passive fast resonant switches

Passive fast resonant switches are bleached by heating caused by γ rays emerging from M_2 (super-luminescence noise or γ-ray lasing) or from M_1. In the simplest case a passive switch is a filament segment of length L_F with an absorption coefficient Σ_F dependent on temperature $T(x, t)$. The temperature distribution $T(x, t)$ parallel to the switch length x obeys

$$\frac{c_V}{\partial t}\frac{\partial T}{\partial t} + \frac{\partial \psi}{\partial x} = 0, \quad \frac{\partial \psi}{\partial x} = -\Sigma_F \psi; \quad \psi = E_\gamma \varphi(x, t), \tag{55}$$

where $\varphi(x, t)$ is the distribution of the γ-ray flux along the filament of length L_F. If $c_V = $ const, it follows from Eq. (55) that the velocity of the temperature front $T(\bar x, \bar t) = \overline T = $ const is

$$d\bar x/d\bar t = \exp\left[-\int_0^{\bar x} \Sigma_F T(x, \bar t)\, dx\right] \psi_0(t)/c_V(\overline T - T_0), \tag{56}$$

where $t = \bar t - \bar x/c'$; $\psi_0(t)$ is the flux of energy ψ at a moment t at the entry to the switch in the plane $x = 0$; $\psi_0(t) = 0$ if $t = \bar t - \bar x/c' < 0$; $\bar x/c'$ is the correction for the delay of the γ-ray wave; T_0 is the initial temperature.

The ideal case corresponds to $\Sigma_F = \Sigma_{F0}$ at temperatures $T < T_F$ and to $\Sigma_F = \Sigma'$ at temperatures $T \geq T_F$ [see Eq. (50)]. Then, the velocity of the bleaching front where $\overline T = T_F$ is

$$v_F = d\bar x/d\bar t = \exp(-\bar x \Sigma') \psi_0(t)/c_V(T_F - T_0). \tag{57}$$

If $\bar x \Sigma' \ll 1$ and $\psi_0(t) = E_\gamma \varphi_0(t) \approx $ const, then for $t > t_1 = (v_F \Sigma_1)^{-1}$, we have

$$\bar x = v_F \bar t - \frac{1}{\Sigma_1}, \quad \Sigma_1 = \Sigma' + \frac{\alpha \varepsilon}{1+\alpha}\Sigma_0, \quad \varepsilon = 1 - \frac{\tau_1}{t_1}\varphi_1\left(\frac{t_1}{\tau_1}\right), \tag{58}$$

where t_1 is the heating time of the front of a fast resonant switch to $T = T_F$ by the photoelectric effect and conversion electrons whose number, relative to the number of resonantly absorbed γ rays, is $\alpha\varepsilon/(1+\alpha)$.

The filament and the fast resonant switch are one and the same crystal, but the concentration of the R nuclei in the switch zone is higher. Usually it is necessary to delay the moment of switching by $\bar t = t_F \gtrsim \tau_1$, but the switching itself should be abrupt and occur in a time $\tau_F \ll \tau_1$, so as to ensure $k(t_F - \tau_F) \ll 1$ and $k(t_F) \approx 1$, where

$$k(t_F - \tau_F) = k_\perp = \exp(-L_i\Sigma_i' - L_f\Sigma_f), \quad k(t_F) = k_\parallel = \exp(-L_i\Sigma_i - L_f\Sigma_f'),$$
$$\Sigma_f' \approx 2\sigma n_f + k_b'\sigma'n', \quad \Sigma_i' \approx 2\sigma n_i + k_b'\sigma'n', \quad n_i < n_f, \quad L_F = L_f + L_i, \tag{59}$$
$$\Sigma_f - \Sigma_f' \approx 2\sigma_0 n_f, \quad \Sigma_i - \Sigma_i' \approx 2\sigma_0 n_i,$$

and the macroscopic γ-ray absorption cross sections $\Sigma \equiv \Sigma_{F0}$ (before bleaching) and Σ' (after bleaching) are given for a B mode [see derivation of Eq. (12)]. Here,

n_i and n_f, Σ_i and Σ_f, Σ_i' and Σ_f', and L_i and L_f are, respectively, the concentrations n, macroscopic cross sections Σ_{F0} and Σ', and lengths L for the initial "delaying"(i) and final "switching" (f) parts of the switch acting as described below.

Radiation flux $\psi_0 = E_\gamma \varphi_0$ of the adjoining part of the filament heats the end (entry) of the switch until the bleaching temperature T_F is reached in a time t_1. Then, the bleaching front travels at a constant velocity $v_F \ll c'$ and passes successively through the delaying section of length L_i and the switching section of length $L_f \ll L_i$. Variation of L_i provides means for controlling the delay time. In the section L_f the concentration of the resonant nuclei is higher and this gives rise to a jump in the absorption by a factor of at least 10 in a time $\tau_F = L_F/v_F$.

By way of example, we shall consider a passive fast resonant switch utilizing the ⁴⁰K nuclei (Table I) in a matrix of the Be type and we shall assume that $k_b' \approx 0.01$ and $T_F - T_0 \approx 500\,°K$. Let us assume that the flux at the entry is $\psi_0 = 5.9 \times 10^{10}$ W/cm²; then, $v_F = 2.4 \times 10^7$ cm/sec. Let the delaying section be $L_i = 0.11$ cm with $n_i = 4.5 \times 10^{20}$ cm⁻³, and the switching section be $L_f = 0.008$ cm with $n_f = 1.3 \times 10^{21}$ cm⁻³. Then, $t_1 = 2.4 \times 10^{-9}$ sec and the total delay time is $t_F = 7.4 \times 10^{-9}$ sec $= 1.2\tau_1$, whereas the switching time is $\tau_F = 3.3 \times 10^{-10}$ sec $= 0.05\tau_1$. The transmission in a time τ_F changes from $k_\perp = 0.096$ (switch nontransmitting) to $k_\parallel = 0.973$ (switch transmitting). A lead shield 0.1 cm thick and 1 cm wide protects a passive or active fast switch from the pump radiation.

B. Hybrid passive—active switches

Synchronization of operation of a passive switch by an external agency (for example, optical laser radiation as in the case of an active switch) can be used in a hybrid passive-active switch with passive delay and active switching, which can be applied to a wide range of nuclei.

C. Applications of fast resonant switches

Fast resonant switches separate physically pumping from lasing, bypassing an unstable intermediate stage since these switches ensure an abrupt change from pumping well below the threshold-when $\mu L' < 1$, there is no superluminescence noise, lasing is weak, and other losses are slight (Fig. 2)- to conditions of strong lasing [Eq. (5)]. We then have $k_{sz}k_u = 1$ [see Eq. (40)] and the threshold pump fluxes for simple fluorescence and decay of lower level schemes are reduced by an order of magnitude to $F_{2r} \approx 10^3 F_e$. Moreover, the conditions (45)–(48) for rf and optical power separation become easier. We can also have a jump from $\mu L' < 1$ to lasing above the threshold when $\xi \gg 1$, $p\xi \gg 10$, $\eta > \eta_e$. Attainment of supercritical conditions corresponding to $p\xi \gg 10$ in very long systems with $\xi \gg 1$ has been regarded as unrealistic because of superluminescence noise and other losses (Fig. 2) and it has not yet been discussed. Fast resonant switches change this situation because they provide means for controlling lasing and optimizing it by programmed operation of a system of switches and a matched change in the distribution of the

pump fluxes along the filament. This ensures conditions of the type encountered in the generation of giant optical pulses and makes threshold conditions much easier.

6. TRAVELING PUMP ZONE. ASYMPTOTIC γ-RAY π PULSE

Let a zone of resonant pumping of length $L_p = c't_p$ travel along an unbounded filament M_2 at a velocity $c' < 3 \times 10^{10}$ cm/sec. In the zeroth approximation a maximum of a pupulation inversion Δ of such a traveling pump zone propagates at the same velocity c'. Let us assume that a resonant photon, acting as a seed of a photon flux φ, appears at the population inversion maximum and travels with it. This photon flux increases mainly at the expense of the inversion maximum, independently of time if initially $\varphi = 0$. Therefore, the flux φ should grow approximately in the same way as in the absence of spontaneous decay. Therefore, a preliminary estimate of the growth of φ can be obtained employing the semiclassical result of Arecchi, Bonifacio, and Hahn (see, for example, Ref. 29), according to which an asymptotic pulse of intensity φ_a forms in an infinitely extended medium and the shape of this pulse

$$\varphi_a(t; x) = \frac{(p-1)^2}{2\tau_2\sigma_0} \text{sech}^2 \left[\frac{(p-1)\tilde{t}}{\tau_2} \right], \quad \tilde{t} = t - t_0 - \frac{x - x_0}{c'}, \quad (60)$$

is independent of the shape of the seed pulse. Here, x is the coordinate along the filament and t_0 is the moment at which the maximum φ_a occurs at the point x_0. The pulse is coherent and it moves at a velocity c'. The result (60) is generalized here, in contrast to the work of Svelto,[29] to the case when $\Delta \neq n_e$. The pulse φ_a alters the population inversion Δ

$$\frac{\Delta(t, x)}{\Delta(-\infty)} = \frac{1}{p} - \left(1 - \frac{1}{p} \right) \text{th} \left[\frac{(p-1)\tilde{t}}{\tau_2} \right], \quad \frac{\Delta(+\infty)}{\Delta(-\infty)} = \frac{2}{p} - 1, \quad (61)$$

where $\Delta(-\infty)$ and $\Delta(+\infty)$ are the values of the inversion at the point x before and after the passage of this pulse. The half-width of the pulse and the integrated flux F_a are

$$t_a = 1.76 \frac{\tau_2}{p-1}, \quad F_a = \int_{-\infty}^{+\infty} \varphi_a(t, x) dt = \frac{p-1}{\sigma_0}. \quad (62)$$

The estimates (60)–(62) are valid if $t_a \ll \tau_1$, i.e., when $p \gg 1$ [see Eq. (62)] when a pulse passes through the point x before the population inversion Δ is lost at this point because of spontaneous decay. However, if a sufficiently short leading edge forms in the course of the growth of the pulse, the pulse is amplified, compressed, and converted into a π pulse.[30] It follows that the use of a traveling pump zone and shortening of the leading edge to $\tau_F \approx 10^{-12}$ sec by a fast resonant switch (Sec. 5) can produce a γ-ray π pulse of duration $t_{\pi a} \gtrsim \tau_F \ll \tau_1$ with a flux $F_\pi \approx F_a$ in a long filament characterized by $\xi \gg 1$ when $p \gtrsim 1$. In this case, fast resonant switches distributed at short intervals along a filament M_2 should operate successively during passage of a population inversion maximum after some optimal delay t_F ($\tau_1 \gg t_F \gg \tau_F$) between this maximum and the leading edge of the pulse φ. Then, the superluminescence noise of the inactive modes, which travel at a different velocity $\mathbf{c}'' \neq \mathbf{c}'$, are removed by the system of switches. The use of this combined traveling pump zone plus fast resonant switch-

ing system in the case of fluorescence or decay of lower level schemes can reduce the pump threshold by two orders of magnitude [see Eq. (40)] to $F_{2a} \approx F_{20}/p_e$ $\approx 70 F_e \approx F_{20}''$ and the combination of a traveling pump zone with fast resonant switches and rf (or optical) pulse separation can reduce the pump threshold to $F_{2a}'' \approx F_{20}''/p_e$ $\approx 10 F_e$, i.e., by three orders of magnitude. The processes in the traveling pump zone with rf (or optical) pulse separation are separated both in time and space: an activation zone of length $L_p = t_p c'$ travels first; it is followed by an rf or optical inversion zone $L_\pi = t_\pi c'$ and by a γ-ray lasing zone (γ-ray π pulse) of length $L_{\gamma\pi}$ $= t_{\pi a} c'$. The threshold conditions attained in this way are then most favorable [see Eq. (40)]:

$$F_{2a}'' \approx 10 F_e \gtrsim 10^{16} \text{ cm}^{-2}, F_{1a}'' \gtrsim 10^{17} \text{ cm}^{-2}, \bar{F}_{1a}'' \gtrsim 10^{19} \text{ cm}^{-2}, F_{1a}'' \cdot \gg 10^{21} \text{ cm}^{-2}.$$

$$(63)$$

A. Annular traveling pump zone schemes

The method of a traveling pump zone is complicated when the length of a filament is considerable: $L \gg L_{ob}$ $\approx 10^2$ cm. However, we shall assume that the filament length is $L \gtrsim 2t_p c'$ and that the traveling pump zone circulates in a loop of radius $R \gtrsim 2d \cot\vartheta/\delta\vartheta \approx 1$ m [ϑ and $\delta\vartheta$ are defined in Eq. (16)] so that a growing γ-ray π pulse follows along the loop in the same way as in a straight filament. Since $t_p \lesssim 5\tau_1$ [see Eq. (43) and Fig. 4], the length of the loop $L \gtrsim 10\tau_1 c'$ is sufficient ($L \gtrsim 1$ m for $\tau_1 \gtrsim 1$ nsec) if in a time $10\tau_1$ the initial temperature of the filament and switches is restored. Since $\tau_s \gtrsim 10^3\tau_1$ [see Eq. (18)], a complete recovery of the distribution of the R nuclei between the hyperfine structure sublevels in a time $t_p \approx 5\tau_1$ since the passage of a pulse is impossible. This should be allowed for by employing fluorescence, decay of lower level, or rf pulse separation schemes. However, this is unimportant in the case of optical pulse separation schemes which are not affected by the hyperfine structure. In the case of some annular rf (or optical) pulse separation schemes a γ-ray π pulse has to be followed by an rf (optical) π pulse in order to restore the traversed section of the filament to a state close to initial.

B. Need for two-stage combined schemes

The two-stage combined scheme considered above (generalized two-stage pumping + anomalous dilution +fast resonant switches +traveling pump zone +optical or rf pulse separation) can be reduced to a one-stage combined scheme by removing the target M_1 and activating the filament M_2 directly. In both one- and two-stage combined schemes we have $p_e \approx 1$ and $\Delta \approx n_e$, and if $\Delta \approx n_e(0) \gtrsim \Delta_b$, we find that Eqs. (6), (13), and (26)–(28) give the activation flux

$$F^{(1)} \approx t_p \Phi_0 \gtrsim \frac{p_e k_b'}{w_e \sigma_0} \frac{\Sigma'}{\Sigma} \frac{t_p}{\tau_1},$$

$$F^{(1)} \gtrsim 10^{14} \text{ cm}^{-2}, F^{(1)} \gtrsim 10^{21} \text{ cm}^{-2}, F^{(1)} \cdot \gg 10^{21} \text{ cm}^{-2}. \quad (64)$$

Thus, direct implantation of R^* in M_2 (see Sec. 3) gives $\bar{F}^{(1)} \ll \bar{F}_{1a}''$. However, it is essential to ensure that the nuclei penetrate to a depth $d \approx 10^{-2}$ cm, i.e., $\Sigma = \bar{\Sigma} \lesssim d^{-1} \approx 10^2$ cm^{-1}. However, this is only possible if the kinetic energy of the ions is $\bar{E} \gtrsim 1$ MeV and a gain μ_0 is destroyed by overheating (see Sec. 1)

$$\delta T \gtrsim \delta T^{(1)} = 4EF^{(1)}/c_V d > 10^3 \,°K, J \gtrsim J^{(1)} = EF^{(1)}/2\tau_i > 10 \; W/cm^{-2}. \qquad (c)$$

This overheating is reduced if the ions are channeled (then $\bar E \ll 1$ MeV) and if $k_b' < 10^{-3}$. However, both these approaches present difficulties at present.

In the case of neutron activation we have $\Sigma_b'/\Sigma \approx 2\sigma/\sigma_t$, $\bar w_e \approx 0.5$, and $\bar F^{(1)} \approx 5.4\sigma/\sigma_e \sigma_T$ (see Table I), and the overheating by the scattering of neutrons on the R' nuclei is

$$\delta T_i^{(1)} = (E/E_T)^{1/2} \bar F^{(1)} \sigma_s' n' \xi_s' E/3\varkappa n' \lesssim 10^2 \,°K^2 \qquad (65)$$

for neutrons of energy $E \lesssim 1$ eV. Here, $\sigma' \approx 6$ b and $\xi_s' \approx 0.24$ are, respectively, the cross section and the mean logarithmic losses in the case of scattering of neutrons by ^{9}Be nuclei.[6] A neutron one-stage combined scheme is consequently possible but less convenient than a two-stage scheme ensuring $\bar F_{1a}'' \approx 7 \times 10^{19}$ cm^{-2} for ^{161}Dy and enabling slowing down to $E \approx 10$ eV without pulverization of M_1 (see Sec. 3) and to $E \approx 10^2 - 10^3$ eV in the case when M_2 is screened from neutrons and the grain size in M_1 is $d_1 \approx \sim 10^{-5} - 10^{-6}$ cm.

One-stage combined schemes are unattainable in the case of Coulomb and γ-ray activation because of overheating amounting to $\delta T > \delta T^{(1)*} \approx E_\gamma^* \Sigma' F^{(1)*}/c_V > 10^5 - 10^6$K, where $E_\gamma^* \gtrsim 10^5$ eV is the energy of the $|e_*\rangle$ level (Sec. 3). Thus, one-stage combined schemes are either much more difficult or quite impossible. Therefore, it is desirable to investigate and particularly simulate (see Sec. 7) two-stage combined schemes, i.e., generalized two-state pumping, although one-stage models are simpler.

7. TABLE OF ACTIVE NUCLEI. PROBLEM γ-RAY LASER. SIMULATION OF GENERALIZED TWO-STAGE PUMPING

We have seen that anomalous dilution and suppression of overheating, generalized two-stage pumping with transfer of the excited nuclei, separation of activation and inversion by rf and optical pulse methods, line narrowing without external action, and control of pumping and γ-ray lasing (by fast resonant switches and traveling pump zone, or their combinations) ensure the easiest threshold and temperature conditions, counteract the losses which can suppress γ-ray lasing, and extend the range of nuclei usable in γ-ray lasers. The six nuclei in Table I do not represent an exhaustive list and may not be even optimal for γ-ray lasing. However, it is clear from this table (for example, in the case of ^{83}Kr) that the $\bar F_{1r} \gtrsim 10^{23}$ cm^{-2} threshold for one of the schemes (traveling pump zone +fast resonant switches +rf or optical pulse separation) with transfer of the R^* nuclei differ by five to six orders of magnitude.

The above analysis makes it clear that in "in situ" difficulties encountered in the pumping and emission from γ-ray lasers can be overcome and that the central problem of γ-ray lasing is different: there is a need for primary activation sources based on such principles as the Coulomb excitation of R nuclei as they traverse a crystal,[21] optical separation of excited nuclei,[7] γ-ray emission by channeled electrons or positrons predicted by Khumakhov,[31] pulsed (in a time of $t \approx 10^{-10}$ sec) emis-

sion of thermal and resonant neutrons from ^{9}Be in a compact region irradiated with synchrotron γ-ray pulses ("neutron focus"[32]).[3] Neutron fluxes predicted by Eremeev[32] can probably be increased by several orders of magnitude by the use of γ-rays emitted by channeled particles.[31] However, some of the key problems in γ-ray lasing can be solved without the use of such sources: long single-block crystals consisting of light atoms and characterized by $k_b' \lesssim 0.01$ can be grown; anomalous dilution can be achieved and it can also be used in the spectroscopy of long-lived isomers; a traveling pump zone and the methods of rf and optical pulse separation can be used in situations other than in γ-ray lasers.

Moreover, it is possible to simulate all the schemes and components of two-stage or one-stage combined methods at longer (for example, optical) wavelengths. This can be done by taking a hollow converter cylinder M_1 and placing inside it a waveguide filament M_2 containing R activator centers excited at the frequency of no-phonon optical transitions (Shpol'skii effect) by the resonant luminescence emitted from M_1 with the following quantum efficiency: $\bar q_1$ in the case of implantation of excited centers in M_1; $\bar q_1$ in the case of a change in the crystallochemical structure of the original R_0 centers excited (by electrons or photons) to a state $|e\rangle$; q_1^* when the same structure is not affected by excitation (see Sec. 3). In simulating fluorescence and rf pulse separation schemes they have to be considered in a generalized manner, replacing if necessary the hyperfine structures of levels (Fig. 3) with levels of the Stark, etc. structures of electronic levels and also replacing an rf π pulse with a π pulse of the corresponding optical frequency. The action of optical fast resonant switches is the same as in Sec. 5 because they are bleached by overheating due to disappearance of no-phonon optical transitions (Shpol'skii effect; analogs of the Mössbauer effect). An asymptotic π pulse in a closed active waveguide filament M_2 (with one of the schemes of the traveling pump zone +fast resonant switches type) can be studied as a long-wavelength analog of a γ-ray π pulse discussed in Sec. 6.

Since systems with a traveling wave zone and fast resonant switches make it possible to avoid the difficulties associated with the fast depletion of the inversion by decay (see Sec. 6), it is natural to expect that long-wavelength analogs (models) or two- or one-stage combined schemes can also operate in the case of transitions which are shorter-lived than in optical lasers and we can thus move from the optical to shorter wavelengths where the main difficulty is the absence of metastable levels. Therefore, we cannot exclude the possibility of another way of solving the γ-ray laser problem by gradual modification of long-wavelength models of one- or two-stage combined schemes into x- or γ-ray lasers.

participants of a seminar at the Moscow State University on the gamm-laser problem held in memory of R. V. Khokhlov.

---

[1] The parameters of the transitions and some of the numerical results are given in Table I (Sec. 7).

[2] In the case of decay to lower level, fluorescence, and one-stage polarized nuclei [V. I. Vysotskiĭ, Zh. Eksp. Teor. Fiz. 77, 492 (1979)-Sov. Phys. 50, 250 (1979)] schemes the lower active level is significantly populated even at the end of the pumping. On the other hand, in the case of rf pulse separation the lower active level remains empty right up to the end of pumping. In the case of optical pulse separation (see Sec. 4d) each nucleus reaching the lower active level does not absorb the generated γ rays, which resembles optical lasing in excimers. If we ignore the losses (Fig. 2), we find that the low-threshold decay of the lower level, fluorescence, polarized nuclei, rf pulse separation, optical pulse separation, combined one-stage, or combined two-stage (Sec. 6b) schemes can be implemented in one or two stages. It is possible to enhance all these schemes by employing combinations designed to ease threshold conditions (Sec. 7).

[3] The method of coherent Coulomb excitation for direct one-stage pumping, suggested by Rivlin, has been developed significantly by V. I. Vysotskiĭ, V. I. Vorontsov, and R. N. Kuz'min [Zh. Eksp. Teor. Fiz. 78, 100 (1980)-Sov. Phys. 51, 49 (1980)]. Here, in the case of generalized two-stage pumping or combined two- and one-stage methods one can recommend a more realistic application: the R^* nuclei evaporated by a scanning electron beam performing coherent Coulomb excitation are implanted in M_1 (generalized two-stage pumping, combined two-stage schemes) or directly in M_2 (one-stage combined schemes) and a form of traveling pump zone if the scanning velocity is c'.

---

[1] L. A. Rivlin, Vopr. Radioelektron. No. 6, 42 (1963).

[2] V. Vali and W. Vali, Proc. IEEE 51, 182, 1248 (1963).

[3] G. C. Baldwin, J. P. Neissel, and L. Tonks, Proc. IEEE 51, 1247 (1963).

[4] R. V. Khokhlov, Pis'ma Zh. Eksp. Teor. Fiz. 15, 580 (1972) [JETP Lett. 15, 414 (1972)].

[5] Yu. A. Il'inskiĭ and R. V. Khokhlov, Zh. Eksp. Teor. Fiz. 65, 1619 (1973) [Sov. Phys. JETP 38, 809 (1974)].

[6] V. I. Gol'danskiĭ and Yu. Kagan, Zh. Eksp. Teor. Fiz. 64, 90 (1973) [Sov. Phys. JETP 37, 49 (1973)].

[7] V. S. Letokhov, Zh. Eksp. Teor. Fiz. 64, 1555 (1973) [Sov. Phys. JETP 37, 787 (1973)].

[8] V. I. Gol'danskiĭ, Yu. Kagan, and V. A. Namiot, Pis'ma Zh. Eksp. Teor. Fiz. 18, 61 (1973) [JETP Lett. 18, 34 (1973)].

[9] V. F. Dmitriev and É. V. Shuryak, Zh. Eksp. Teor. Fiz. 67, 494 (1974) [Sov. Phys. JETP 40, 244 (1975)].

[10] Tz. Bonchev and P. Kamenov, Bulg. J. Phys. 2, 425 (1975).

[11] G. C. Baldwin and R. V. Khokhlov, Phys. Today 28, No. 2, 32 (1975).

[12] B. V. Chirikov, Zh. Eksp. Teor. Fiz. 44, 2016 (1963) [Sov. Phys. JETP 17, 1355 (1963)].

[13] V. I. Borontsov and V. I. Vysotskiĭ, Zh. Eksp. Teor. Fiz. 66, 1528 (1974) [Sov. Phys. JETP 39, 748 (1974)].

[14] G. T. Trammell and J. P. Hannon, Opt. Commun. 15, 325 (1975).

[15] A. V. Andreev, Yu. A. Il'inskiĭ, and R. V. Khokhlov, Zh. Eksp. Teor. Fiz. 73, 1296 (1977) [Sov. Phys. JETP 46, 682 (1977)].

[16] A. V. Andreev, Kandidatskaya dissertatsiya (Thesis for Candidate's Degree), Moscow State University, 1978.

[17] O. V. Lounasmaa, Experimental Principles and Methods Below One Degree Kelvin, Academic Press, New York, 1974 (Russ. Transl., Mir, M., 1977), Chap. 9.

[18] V. I. Iveronova and G. P. Revkevich, Teoriya rasseyaniya rentgenovskikh lucheĭ (Theory of X-Ray Scattering), Moscow State University, 1978, Chap. 12.

[19] A. Abragam, The Principles of Nuclear Magnetism, Clarendon Press, Oxford, 1961 (Russ. Transl., IIL, M., 1963), Chap. 9.

[20] S. A. Al'tshuler and B. M. Kozyrev, Élektronnyĭ paramagnitnyĭ rezonans, Nauka, M., 1972, Appendix 4 (Electron Paramagnetic Resonance, Academic Press, New York, 1964).

[21] V. A. Bushuev, A. V. Kolpakov, R. N. Kuz'min, E. M. Saprykin, and D. A. Shalabaev, Vestn. Mosk. Univ. Fiz. Astron. 19, 101 (1978).

[22] V. S. Letokhov, Kvantovaya Elektron. (Moscow) No. 4, 125 (1973) [Sov. J. Quantum Electron. 3, 360 (1974)].

[23] G. E. Bizina, A. G. Beda, N. A. Burgov, and A. V. Davydov, Zh. Eksp. Teor. Fiz. 45, 1408 (1963) [Sov. Phys. JETP 18, 973 (1964)].

[24] A. Maitland and M. H. Dunn, Laser Physics, North-Holland, Amsterdam, 1969 (Russ. Transl. Nauka, M., 1978), Chap. 3.

[25] E. F. Makarov and A. V. Mitin, Usp. Fiz. Nauk 120, 55 (1976) [Sov. Phys. Usp. 19, 741 (1976)].

[26] S. V. Karyagin, Pis'ma Zh. Tekh. Fiz. 2, 500 (1976) [Sov. Tech. Phys. Lett. 2, 196 (1976)].

[27] S. V. Karyagin, Proc. Intern. Conf. on Mössbauer Spectroscopy, Bucharest, 1977, Vol. 2, p. 1.

[28] G. V. H. Wilson, Appl. Phys. Lett. 30, 213 (1977).

[29] O. Svelto, Principles of Lasers, Plenum Press, New York, 1976 (Russ. Transl., Mir, M., 1979), Chap. 9.

[30] P. G. Kryukov and V. S. Letokhov, Usp. Fiz. Nauk 99, 169 (1969) [Sov. Phys. Usp. 12, 641 (1970)].

[31] M. A. Kumakhov, Zh. Eksp. Teor. Fiz. 72, 1489 (1977) [Sov. Phys. JETP 45, 781 (1977)].

[32] I. P. Eremeev, Pis'ma Zh. Eksp. Teor. Fiz. 27, 13 (1978) [JETP Lett. 27, 10 (1978)].

[33] D. Barband and M. Morariu, "Decay schemes and parameters on Mössbauer isotopes," Preprint NP-2-1978, Bucharest-Magurele, 1978.

Translated by A. Tybulewicz

381   Sov. Phys. JETP 52(3), Sept. 1980

S. V. Karyagin   381